Bioorganic Chemistry 89 (2019) 102995

Contents lists available at ScienceDirect

Bioorganic Chemistry

journal homepage: www.elsevier.com/locate/bioorg

Cytotoxic diterpenoids as potential anticancer agents from the twigs of *Casearia kurzii*

Feng Liu[a], Qi Zhang[a], Xueyuan Yang[a], Yaru Xi[a], Xuke Zhang[a], Huimei Wang[a], Jie Zhang[b], Muhetaer Tuerhong[c], Da-Qing Jin[d], Dongho Lee[e], Jing Xu[a,f,*], Yasushi Ohizumi[g], Ling Shuai[a], Yuanqiang Guo[a,*]

[a] State Key Laboratory of Medicinal Chemical Biology, College of Pharmacy, and Tianjin Key Laboratory of Molecular Drug Research, Nankai University, Tianjin 300350, People's Republic of China
[b] Key Laboratory for Green Processing of Chemical Engineering of Xinjiang Bingtuan, School of Chemistry and Chemical Engineering, Shihezi University, Shihezi 832003, People's Republic of China
[c] College of Chemistry and Environmental Sciences, Laboratory of Xinjiang Native Medicinal and Edible Plant Resources Chemistry, Kashgar University, Kashgar 844000, People's Republic of China
[d] School of Medicine, Nankai University, Tianjin 300071, People's Republic of China
[e] Department of Biosystems and Biotechnology, College of Life Sciences and Biotechnology, Korea University, Seoul 02841, Republic of Korea
[f] State Key Laboratory for Chemistry and Molecular Engineering of Medicinal Resources, Guangxi Normal University, People's Republic of China
[g] Kansei Fukushi Research Institute, Tohoku Fukushi University, Sendai 989-3201, Japan

ARTICLE INFO

Keywords:
Clerodane diterpenoids
Cytotoxic activities
Casearia kurzii
Apoptosis
Cell cycle

ABSTRACT

A search for bioactive natural products as anticancer lead compounds has led to the isolation of five new clerodane diterpenoids (**1**–**5**) from the twigs of *Casearia kurzii*. Their structures were elucidated by extensive analysis of their NMR, IR, and HRESIMS data, and the absolute configurations were determined by experimental and calculated electronic circular dichroism (ECD) data analysis. The isolates were biologically evaluated and showed cytotoxic activities toward human lung cancer cells (A549), human cervical cancer cells (HeLa), and human hepatocellular carcinoma cells (HepG2). The most active compound (**5**) with an IC_{50} value of 5.3 μM against HeLa cells, was found to induce apoptosis and arrest the HeLa cell cycle at G0/G1 stage to exert cytotoxic effects.

1. Introduction

Natural products have played an important role in research and development of new pharmaceuticals and many drugs are derived from natural products or natural product derivatives [1]. Among natural products, diterpenoids are a large group of compounds that have been found from many higher plants. Plants of the genus *Casearia*, belonging to the Flacourtiaceae plant family, consist of about 160 species and are distributed widely in tropical Africa, Asia, northwest Australia, and South America [2]. Some species of this genus have been used as folk medicines for multiple medical indications [3]. Recent phytochemical investigations have also shown the genus *Casearia* to be a rich source of terpenoids, especially diterpenoids, which show various biological effects, such as antimalarial, cytotoxic, antimicrobial, antifungal, neurite outgrowth promoting, and DNA-modifying activities [3–11].

The species *Casearia kurzii* C. B. Clarke is a small tree growing mainly in Yunnan Province of mainland China, India, and northern Myanmar. There are no records on its traditional medicinal uses in Chinese medical texts and no phytochemical reports on its chemical constituents. Considering the applications of some *Casearia* species as folk medicines and the discovery of their bioactive constituents, the chemical constituents of the twigs of *C. kurzii* were investigated during a search for bioactive substances from plants. This investigation led to the isolation of five new clerodane diterpenoids (**1**–**5**) (Fig. 1). The structures of compounds **1**–**5** were established by a combination of NMR, MS, and electronic circular dichroism (ECD) data analysis. The isolated compounds were evaluated for their cytotoxic activities against human lung cancer cells (A549), human cervical cancer cells (HeLa), and human hepatocellular carcinoma cells (HepG2). The most active compound (**5**) was selected to investigate its cytotoxic mechanism against HeLa cells. Herein, the isolation, structural elucidation, and cytotoxic effects of diterpenoids (**1**–**5**) as well as their preliminary

* Corresponding authors.
E-mail addresses: xujing611@nankai.edu.cn (J. Xu), victgyq@nankai.edu.cn (Y. Guo).

https://doi.org/10.1016/j.bioorg.2019.102995
Received 24 January 2019; Received in revised form 4 April 2019; Accepted 17 May 2019
Available online 23 May 2019
0045-2068/ © 2019 Elsevier Inc. All rights reserved.

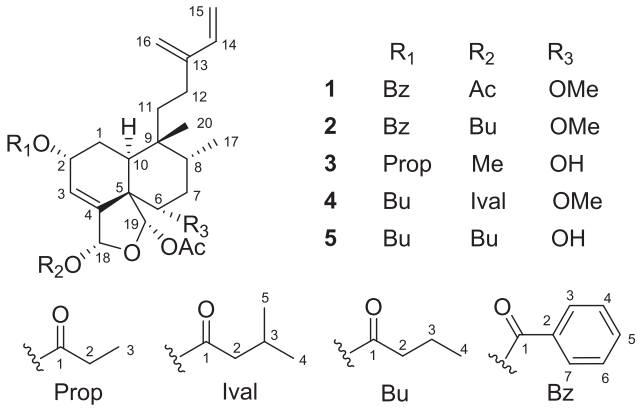

Fig. 1. Structures of compounds **1**–**5**.

action mechanism are described.

2. Experimental

2.1. General experimental procedures

Optical rotations were recorded on an InsMark IP120 automatic polarimeter (InsMark Instrument Co., Ltd., Shanghai, People's Republic of China). ECD spectra were obtained on a JASCO J-715 CD spectrometer (JASCO Corporation, Tokyo, Japan). Infrared (IR) spectra (KBr disks) were recorded on a Bruker Tensor 27 FT-IR spectrometer. 1D and 2D NMR experiments were performed on a Bruker AV 400 instrument (Bruker, Switzerland, 100 MHz for ^{13}C and 400 MHz for ^{1}H) with TMS as an internal reference at room temperature. ESIMS and HRESIMS data were acquired on a Thermo Finnigan LCQ-Advantage mass spectrometer and an IonSpec 7.0 T FTICR MS (IonSpec Co., Ltd., Lake Forest, CA), respectively. HPLC separations were conducted on a CXTH system, equipped with a Shodex RI-102 detector (Showa Denko Co., Ltd., Tokyo, Japan) and a YMC-pack ODS-AM (20 × 250 mm) column (YMC Co. Ltd., Kyoto, Japan). Medium-pressure liquid chromatography (MPLC) was run on a P0100 pump with an ultraviolet (UV) detector (Huideyi Co., Beijing, People's Republic of China) and a column (40 × 400 mm) filled by octadecylsilyl (ODS, 50 μm, YMC Co., Ltd.). Silica gel (200–300 mesh) used for column chromatography was purchased from Qingdao Haiyang Chemical Group Co., Ltd. (Qingdao, People's Republic of China). Chemical reagents (analytical grade) and biological reagents were provided by Tianjin Chemical Reagent Co. (Tianjin, People's Republic of China) and Sigma Co., respectively. The A549, HeLa, and HepG2 cell lines were purchased from Shanghai Institutes for Biological Sciences, Chinese Academy of Sciences (Shanghai, People's Republic of China).

2.2. Plant material

The twigs of *Casearia kurzii* were collected from Xishuangbanna, Yunnan Province, People's Republic of China, in May 2015. The botanical identification was made by one of the authors (Y. Guo). A voucher specimen (No. 20150509) was deposited at the laboratory of bioactive substances and functions of natural medicines, College of Pharmacy, Nankai University.

2.3. Extraction and isolation

The air-dried twigs of *C. kurzii* (31.0 kg) were extracted with MeOH (3 × 186 L) under reflux. The organic solvent was evaporated to afford a crude extract (1400 g), which was suspended in H_2O (1.4 L) and then partitioned with ethyl acetate (6 × 1.4 L) to give the ethyl acetate-soluble portion (318 g). This portion was fractionated by silica gel column chromatography (silica gel, 1.0 kg; column, 9 × 70 cm), using a gradient solvent system of petroleum ether-acetone (100: 0, 100: 2, 100: 4, 100: 6, 100: 8, 100: 11, 100: 16, 100: 22, 100: 30, 100: 40, 21 L for each gradient elution), to afford nine fractions (F_1–F_9) according to TLC analysis. Fraction F_5 was subjected to MPLC over ODS eluting with a step gradient of 65–92% MeOH in H_2O to give ten subfractions $F_{5\text{-}1}$–$F_{5\text{-}10}$. The subsequent purification of $F_{5\text{-}8}$ (87% MeOH in H_2O) by preparative HPLC (YMC-pack ODS-AM, 250 × 20 mm) resulted in the isolation of compound **1** (t_R = 31.8 min, 15.0 mg). Fraction F_4, with the same procedure as for fraction F_5, gave eight subfractions $F_{4\text{-}1}$–$F_{4\text{-}8}$. Using the above HPLC system, compounds **2** (t_R = 39.3 min, 2.0 mg) and **4** (t_R = 35.8 min, 10.6 mg) were isolated from $F_{4\text{-}7}$ (89% MeOH in H_2O). Using the same protocol as for F_4, fraction F_6 yielded six subfractions $F_{6\text{-}1}$–$F_{6\text{-}6}$. The subsequent purification of $F_{6\text{-}4}$ (85.5% MeOH in H_2O) led to the isolation of compound **5** (t_R = 32.7 min, 8.8 mg) by the above-mentioned HPLC procedure. $F_{6\text{-}2}$ was difficult to purify by HPLC and was thus subjected to MPLC again eluting with a step gradient from 68–84% MeOH in H_2O to give six subfractions $F_{6\text{-}2\text{-}1}$–$F_{6\text{-}2\text{-}6}$. Subsequently, the purification of $F_{6\text{-}2\text{-}2}$ (77.5% MeOH in H_2O) using the same HPLC system yielded compound **3** (t_R = 44.8 min, 4.9 mg).

*Kurziterpene A (**1**):* colorless oil; [α] +7.4 (*c* 0.5, CH_2Cl_2); ECD (CH_3CN) 204 (Δε +23.5), 218 (Δε +3.8), 231 (Δε +10.3) nm; IR ν_{max} 2964, 2930, 1753, 1714, 1268, 1224, 1174, 1098, 1068, 948, 923, 894, 668 cm^{-1}; ^{1}H NMR (400 MHz, $CDCl_3$) and ^{13}C NMR (100 MHz, $CDCl_3$) data, see Tables 1 and 2; ESIMS *m/z* 575 $[M+Na]^+$; HRESIMS *m/z* 575.2620 $[M+Na]^+$, calcd for $C_{32}H_{40}NaO_8$, 575.2621.

*Kurziterpene B (**2**):* colorless oil; $[\alpha]_D^{22}$ −7.2 (*c* 0.1, CH_2Cl_2); ECD (CH_3CN) 204 (Δε +16.7), 219 (Δε +2.7), 232 (Δε +7.2) nm; IR ν_{max} 2961, 2927, 2876, 1748, 1716, 1461, 1372, 1315, 1265, 1098, 1066, 948, 924, 895, 734, 715 cm^{-1}; ^{1}H NMR (400 MHz, $CDCl_3$) and ^{13}C NMR (100 MHz, $CDCl_3$) data, see Tables 1 and 2; ESIMS *m/z* 603 [M

Table 1
^{13}C NMR data for compounds **1**–**5** (100 MHz, δ in ppm).

Position		1	2	3	4	5
1		27.3	27.2	27.1	27.0	26.8
2		67.1	67.2	66.2	66.4	66.3
3		121.2	121.2	121.7	121.2	121.8
4		146.5	146.8	146.3	146.3	145.5
5		53.2	53.3	53.6	53.0	53.7
6		81.8	81.8	73.3	81.9	73.1
7		31.1	31.1	37.3	31.1	37.1
8		36.7	36.7	37.3	36.9	37.4
9		37.5	37.5	37.3	37.5	37.4
10		37.0	37.0	36.6	36.4	36.5
11		27.8	27.8	28.2	27.7	28.0
12		23.9	23.9	23.8	23.7	23.7
13		145.1	145.1	145.3	145.1	145.1
14		140.5	140.5	140.3	140.5	140.4
15		112.2	112.1	112.4	112.2	112.3
16		115.6	115.6	115.3	115.6	115.5
17		15.9	15.9	15.7	15.9	15.7
18		96.1	95.9	104.7	95.9	95.4
19		98.3	98.3	97.6	98.4	97.9
20		25.7	25.7	25.4	25.5	25.4
OR-2[a]	1	165.8	165.8	174.0	172.5	173.1
	2	130.6	130.6	27.9	36.4	36.5
	3/7	129.6	129.6	9.2	18.3	18.7
	4/6	128.5	128.5		13.6	13.5
	5	133.2	133.1			
OR-6[a]	1	57.5	57.5		57.5	
OR-18[a]	1	170.3	172.9	56.3	172.8	172.6
	2	21.7	36.4		43.7	36.3
	3		18.3		26.1	18.3
	4		13.5		22.4	13.6
	5				22.4	
OR-19[a]	1	169.8	169.8	170.3	169.8	169.7
	2	21.4	21.6	21.6	21.6	21.4

[a] A number with a superscript indicates the location of the substituent group in the parent skeleton.

Table 2
^{1}H NMR data for data for compounds **1–5** (400 MHz, δ in ppm, J in Hz).

Position		1	2	3	4	5
1α		2.06 m	2.07 m	1.97 m	1.72 m	1.71 m
1β		1.73 m	1.97 m	1.86 m	1.95 m	1.92 m
2		5.70 br s	5.69 br s	5.48 br s	5.43 br s	5.45 br s
3		6.06 d (3.7)	6.05 d (4.0)	6.06 d (2.7)	5.95 d (3.9)	5.99 d (3.7)
6		3.36 dd (3.4, 12.0)	3.38 dd (3.4, 12.0)	3.76 dd (4.5, 11.3)	3.32 dd (3.9, 12.0)	3.79 dd (4.4, 11.6)
7α		1.89 m	1.88 m	1.76 m	1.86 m	1.65 m
7β		1.53 m	1.42 m	1.66 m	1.52 m	1.73 m
8		2.47 m	2.47 m	1.70 m	1.70 m	1.71 m
10		1.74 m[b]	1.74 m[b]	2.27 dd (12.9, 3.9)	2.09 m[b]	2.32 m[b]
11		1.26 m	1.28 m	2.38 m	1.27 m	1.23 m
		1.53 m	1.44 m	2.09 m	1.48 m	1.52 m
12		2.13 m	2.12 m	2.08 m	2.08 m	2.09 m
14		6.45 dd (11.0, 17.4)	6.45 dd (10.0, 17.8)	6.43 dd (11.0, 17.6)	6.46 dd (10.8, 17.5)	6.44 dd (10.5,17.6)
15		5.20 d (17.4)	5.20 d (17.8)	5.19 d (17.6)	5.20 d (17.5)	5.20 d (17.6)
		5.04 d (11.0)	5.04 d (10.0)	5.03 d (11.0)	5.05 d (10.8)	5.04 d (10.5)
16		5.06 br s	5.06 br s	5.05 s	5.05 br s	5.05 br s
		4.96 br s	4.96 br s	4.94 s	4.94 br s	4.95 br s
17		0.97 d (8.5)	0.96 d (9.1)	0.93 d (5.8)	0.95 d (6.8)	0.93 d (6.7)
18		6.69 s	6.71 s	5.48 br s	6.68 s	6.75 br s
19		6.47 s	6.46 s	6.46 br s	6.43 s	6.48 br s
20		0.95 s	0.95 s	0.92 s	0.95 s	0.93 s
OR-2[a]	2			2.38 q (7.7)	2.34 m	2.36 t (7.3)
	3/7	8.08 d (7.4)	8.06 d (7.3)	1.17 t (7.7)	1.65 m	1.65 m
	4/6	7.48 t (7.4)	7.48 t (7.3)		0.94 t (7.5)	1.00 t (7.4)
	5	7.61 t (7.4)	7.61 t (7.3)			
OR-6[a]		3.33 s	3.33 s		3.30 s	
OR-18[a]	2	1.90 s	2.28 t (7.4)	3.44 s	2.30 m	2.30 t (7.3)
	3		1.59 m		2.12 m	1.67 m
	4		0.89 t (7.4)		1.02 d (6.4)	0.93 t (7.4)
	5				1.03 d (6.4)	
OR-19[a]		2.06 s	1.89 s	1.90 s	1.86 s	1.89 s

[a] A number with a superscript indicates the location of the substituent group in the parent skeleton.
[b] Signals are in overlapped regions of the spectra, and the multiplicities could not be discerned.

$+Na]^+$; HRESIMS m/z 603.2932 $[M+Na]^+$, calcd for calcd for $C_{34}H_{44}NaO_8$, 603.2937.

Kurziterpene C ***(3)****:* colorless oil; $[\alpha]_D^{23}$ +22.7 (*c* 0.2, CH_2Cl_2); ECD (CH_3CN) 201 ($\Delta\varepsilon$ +10.3), 226 ($\Delta\varepsilon$ −1.5) nm; IR ν_{max} 3484, 2954, 2925, 2856, 1731, 1422, 1373, 1223, 1172, 1080, 1041, 1006, 946, 894 cm^{-1}; ^{1}H NMR (400 MHz, $CDCl_3$) and ^{13}C NMR (100 MHz, $CDCl_3$) data, see Tables 1 and 2; ESIMS m/z 485 $[M+Na]^+$; HRESIMS m/z 485.2512 $[M+Na]^+$, calcd for $C_{26}H_{38}NaO_7$, 485.2515.

Kurziterpene D ***(4)****:* colorless oil; $[\alpha]_D^{23}$ +0.6 (*c* 0.3, CH_2Cl_2); ECD (CH_3CN) 202 ($\Delta\varepsilon$ +17.3), 227 ($\Delta\varepsilon$ −0.27), 228 ($\Delta\varepsilon$ −0.25) nm; IR ν_{max} 2962, 2932, 1748, 1727, 1457, 1264, 1220, 1169, 1097, 1063, 946, 936, 733, 702 cm^{-1}; ^{1}H NMR (400 MHz, $CDCl_3$) and ^{13}C NMR (100 MHz, $CDCl_3$) data, see Tables 1 and 2; ESIMS m/z 583 $[M+Na]^+$; HRESIMS m/z 583.3245 $[M+Na]^+$, calcd for $C_{32}H_{48}NaO_8$, 583.3247.

Kurziterpene E ***(5)****:* colorless oil; $[\alpha]_D^{26}$ +22.2 (*c* 0.5, CH_2Cl_2); ECD (CH_3CN) 203 ($\Delta\varepsilon$ +12.7), 231 ($\Delta\varepsilon$ −0.1), 239 ($\Delta\varepsilon$ +0.3) nm; IR ν_{max} 3513, 2964, 2931, 1750, 1729, 1371, 1249, 1220, 942, 891, 734, 702 cm^{-1}; ^{1}H NMR (400 MHz, $CDCl_3$) and ^{13}C NMR (100 MHz, $CDCl_3$) data, see Tables 1 and 2; ESIMS m/z 555 $[M+Na]^+$; HRESIMS m/z 555.2932 $[M+Na]^+$, calcd for $C_{30}H_{44}NaO_8$, 555.2934.

2.4. Computational method

Geometry optimizations, re-optimizations, ECD calculations, and simulations were conducted according to the method reported previously [9–14].

2.5. Cytotoxic activity assay

The cytotoxic activities were evaluated using a MTT assay. Cells were cultured in RPMI-1640 (A549 and HeLa cells) or DMEM (HepG2 cells) medium supplemented with 10% (v/v) fetal bovine serum and 100 U/mL penicillin/streptomycin under a water-saturated atmosphere of 95% air and 5% CO_2. After reaching approximately 80% confluence, the cells were harvested and seeded in 96-well plates (1×10^4 cells/well) and allowed to adhere for 24 h at 37 °C. Then, cells were treated with the test samples dissolved in DMSO at different concentrations, including the positive and the negative controls. Etoposide was used as a positive control. After a continuous incubation for 48 h, 20 μL MTT solution (5 mg/mL, Solarbio, Beijing, People's Republic of China) were added in each well for 4 h. Then, the medium was replaced with 150 μL DMSO and the absorbance was measured at 492 nm using microplate reader (Thermo Fisher Scientific Inc. America). The experiments were performed in triplicate, and the IC_{50} value was defined as the concentration of the compounds that inhibited cell proliferation by 50%.

2.6. Apoptosis analysis by flow cytometry

Cell apoptosis was analyzed by flow cytometry using Annexin V-FITC Apoptosis Detection Kit (Beyotime, Shanghai, People's Republic of China) according to the manufacturer's instruction. Briefly, HeLa cells were treated with various concentrations (2.5, 5, and 10 μM) of the test compound. After an incubation of 48 h, the cells were washed twice with PBS and resuspended in the binding buffer (Beyotime). This suspension was incubated for 20 min at room temperature in the dark after adding 5 μL Annexin V-FITC and 10 μL PI. Then, cell apoptosis was examined by BD LSRFortessa flow cytometry (BD Biosciences). The cell apoptosis data have been obtained with FLOWJO flow cytometry analysis software (FLOWJO LLC, Ashland, OR, USA).

2.7. Cell cycle analysis

Flow cytometric analysis was performed to evaluate the distribution of the cell cycle. HeLa cells (2×10^5 cells/well) in exponential growth phase were treated with different concentrations (2.5, 5, and 10 μM) of

the selected compound. After an exposure to the test sample for 48 h, the cells were harvested, washed with PBS twice, and fixed in 70% ice-cold ethanol at 4 °C overnight. Then, the cells were washed with PBS twice and treated with propidium iodide staining buffer containing RNase (Beyotime) for 30 min at 37 °C, followed immediately by cellar DNA analysis using BDLSR Fortessa flow cytometry. Data were processed using ModFit LT Software.

3. Results and discussion

3.1. Structure elucidation

Fractionation of the ethyl acetate-soluble part of the methanol extract of the twigs of *C. kurzii* yielded five previously undescribed diterpenoids (**1–5**).

Compound **1** was obtained as a colorless oil. Its HRESIMS suggested a molecular formula of $C_{32}H_{40}O_8$ through the presence of a peak at *m/z* 575.2620 $[M+Na]^+$ (calcd for $C_{32}H_{40}NaO_8$, 575.2621), which was consistent with its NMR data (Tables 1 and 2). From the ^{1}H NMR spectrum of **1**, a set of aromatic proton signals [δ_H 8.08 (2H, d, J = 7.4 Hz), 7.48 (2H, t, J = 7.4 Hz), 7.61 (1H, t, J = 7.4 Hz)], one methoxy singlet (δ_H 3.33), and two acetyl methyl singlets (δ_H 1.90 and 2.06) were observed. These characteristic proton signals, together with the corresponding carbon signals (δ_C 165.8, 130.6, 129.6 × 2, 128.5 × 2, 133.2, 57.5, 170.3, 21.7, 169.8, and 21.4), suggested the presence of one benzoyloxy, one methoxy, and two acetyloxy groups in compound **1** [8–11]. Excluding the signals for these substituent groups, there were additional 20 carbons displayed in the ^{13}C NMR spectrum of **1**. These 20 typical skeletal carbons, especially the two acetal (δ_C 96.1 and 98.3) and four olefinic carbons (δ_C 112.2, 115.6, 140.5, and 145.1) forming two terminal double bonds, implied that compound **1** is a clerodane-type diterpenoid, according to similar substances reported previously from the genus *Casearia* [8–11]. The structure of the clerodane-type diterpenoid (**1**) was elucidated and confirmed as shown in Fig. 2 by HMBC and ^{1}H–^{1}H COSY experiments. By analyzing its 2D NMR spectra, the olefinic, acetal, and oxygenated carbon signals at δ_C 121.2 (C-3), 146.5 (C-4), 145.1 (C-13), 140.5 (C-14), 112.2 (C-15), 115.6 (C-16), 96.1 (C-18), 98.3 (C-19), 67.1 (C-2), and 81.8 (C-6) were assigned, and detailed analysis of the 1D and 2D NMR data allowed the other carbon and proton signals to be attributed. Use of the long-range couplings observed in the HMBC spectrum permitted the placement of the above substituent groups. The benzoyloxy group was demonstrated to be attached at C-2 by the HMBC correlation of H-2 (δ_H 5.70) to the carbonyl carbon (δ_C 165.8) of the benzoyloxy group. Similarly, the methoxy group located at C-6, and the two acetyloxy groups located at C-18 and C-19, were also determined by the corresponding HMBC correlations of the skeletal protons to the corresponding carbons (Fig. 2). The planar structure of **1** was therefore elucidated as illustrated in Fig. 2.

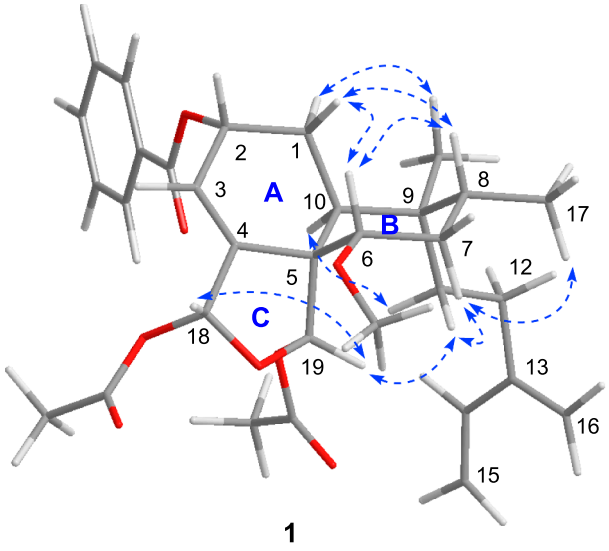

Fig. 3. Conformation and key NOESY correlations of compound **1**.

The relative configuration of compound **1** was established based on its NOESY spectrum and Chem3D molecular modeling. NOESY

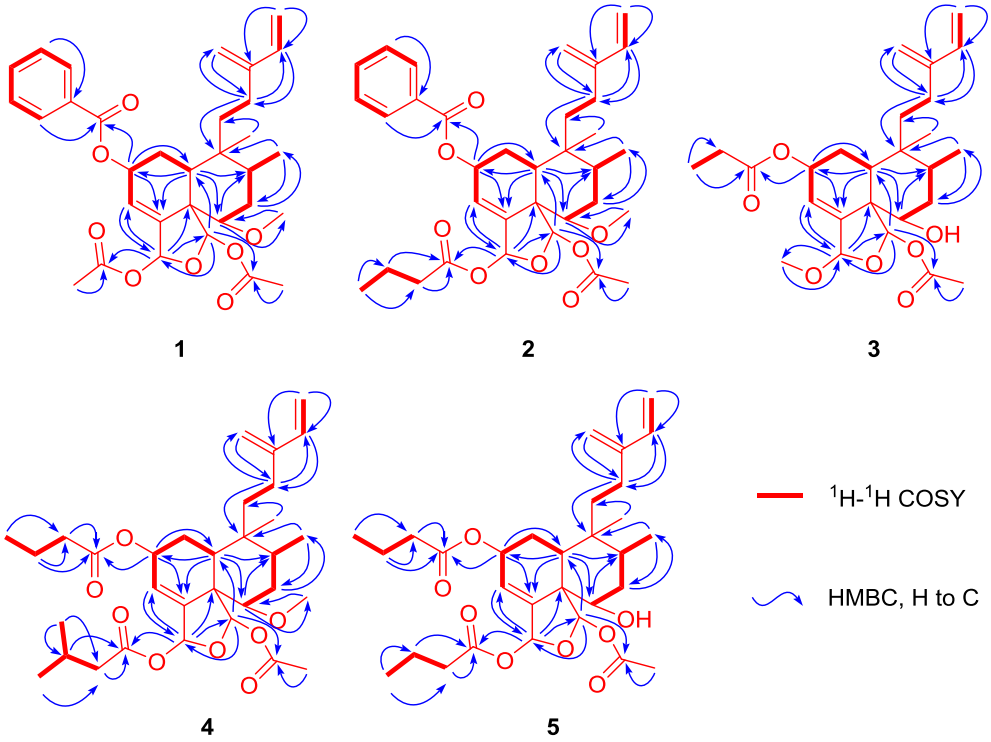

Fig. 2. ^{1}H–^{1}H COSY and key HMBC correlations of compounds **1–5**.

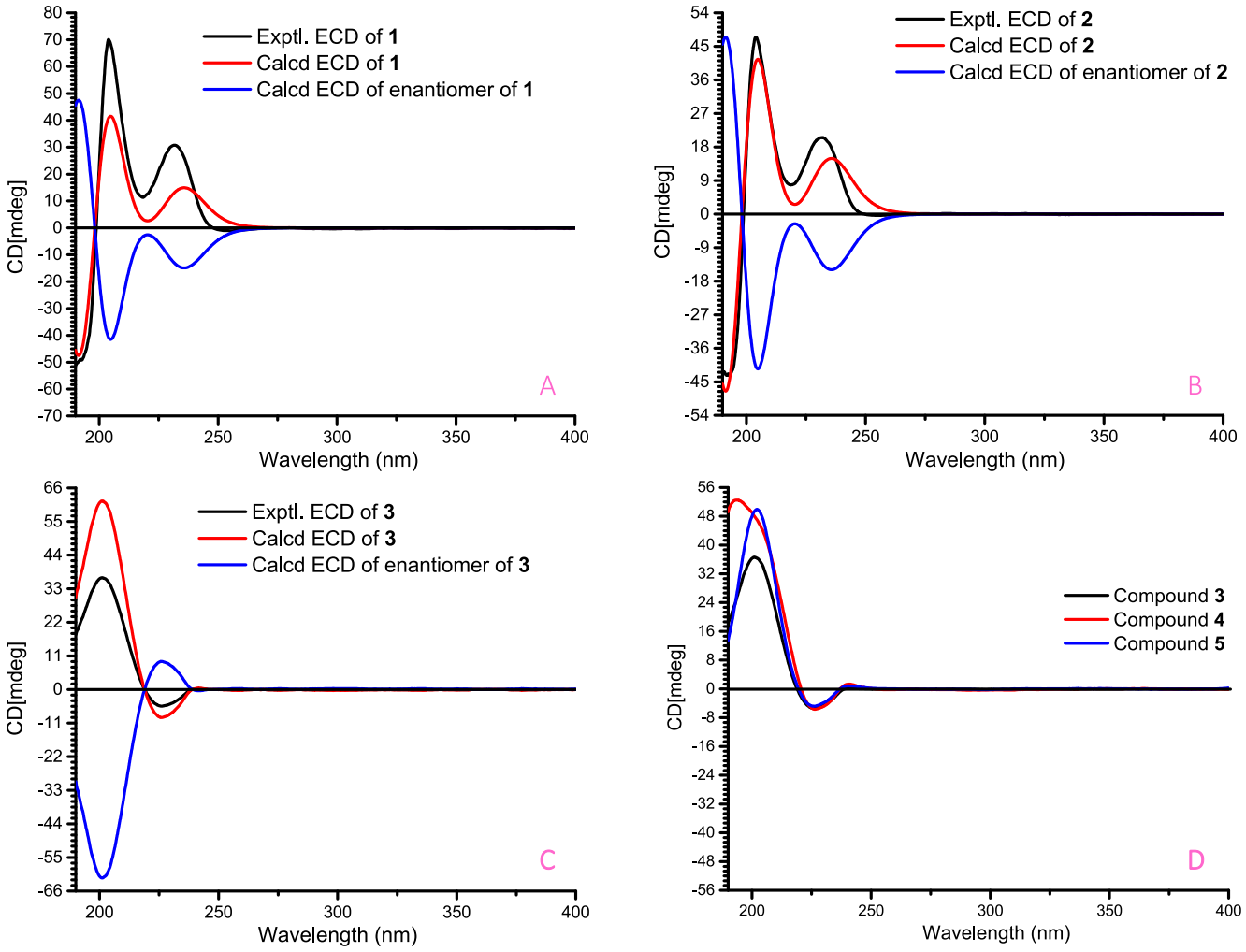

Fig. 4. Calculated and/or experimental ECD spectra of compounds **1** (A), **2** (B), **3** (C), **4** (D), and **5** (D) in acetonitrile.

correlations observed for H-1β/H-8, H-8/H-6, H-1β/H-6, H-18/H-19, H-19/H_2-11, H-19/H-7α, H-7α/H_2-11, H-7α/H_3-17, and H-10/H_2-11, together with the Chem3D modeling, suggested a conformation for compound **1** as depicted in Fig. 3. According to these NOESY correlations, two six-membered rings are *cis*-fused with H-10 and C-19 both in α-positions, ring A is shown to have a twisted chair conformation with an α-orientation for the C-2 benzoyloxy group, ring B has a normal chair conformation with H-6 β-axially oriented, Me-17 is α-equatorially oriented, and Me-20 β-equatorially oriented, while ring C exhibits an envelope conformation with β-orientations for both H-18 and H-19. After defining the relative configuration, the absolute configuration of **1** was established by time-dependent density functional theory (TDDFT) ECD calculations [10,11]. Starting from the conformation of **1** deduced from the NOESY correlations and Chem3D modeling, conformational searches with the MMFF94S force field by MOE software and geometry optimizations by the Gaussian 09 package were performed. Then, the ECD spectra were calculated at the CAM-B3LYP/SVP level with the CPCM model in acetonitrile. The obtained ECD spectrum of **1** matched the experimental data closely (Fig. 4A), which suggested a (2*R*,5*S*,6*S*,8*R*,9*R*,10*S*,18*R*,19*S*) absolute configuration for compound **1**. All of the above evidence allowed the structure of **1** to be established as (2*R*,5*S*,6*S*,8*R*,9*R*,10*S*,18*R*,19*S*)-2-benzoyloxy-6-methoxy-18,19-diacetyloxy-18,19-epoxycleroda-3,13(16),14-triene, which has been named kurziterpene A.

The molecular formula of compound **2** (kurziterpene B) was determined as $C_{34}H_{44}O_8$ based on the HRESIMS (*m/z* 603.2932 $[M+Na]^+$, calcd for $C_{34}H_{44}NaO_8$, 603.2937). Its ^1H and ^{13}C NMR spectra resembled those of compound **1** closely, which implied that **2** is also be a clerodane diterpenoid. According to their ^1H and ^{13}C NMR data, the main difference observed between compounds **2** and **1** is that one acetyloxy group in **1** is replaced by a butyryloxy group (δ_C 172.9, 36.4, 18.3, and 13.5) in **2**, which was supported by the 2D NMR data. Following the confirmation of the framework and the substituent groups of **2** by the interpretation of 2D NMR spectra, the locations of one benzoyloxy, one acetyloxy, one methoxy, and one butyryloxy group were determined using the HMBC data (Fig. 2). The long-range correlations of H-2 (δ_H 5.69), H-18 (δ_H 6.71), and H-19 (δ_H 6.46) to the corresponding carbonyls (δ_C 165.8, 172.9, and 169.8) of the acyloxy groups revealed that the benzoyloxy, the butyryloxy, and the acetyloxy group, are located at C-2, C-18, and C-19, respectively. The methoxy group could only be attached to C-6, as confirmed by the HMBC couplings of H-6 (δ_H 3.38) to the methoxy carbon (δ_C 57.5). The scaffold conformation of **2** was deduced to be the same as that of compound **1**, where the C-2 benzoyloxy, the C-6 methoxy, the C-18 butyryloxy, and the C-19 acetyloxy groups were all found to be α-oriented as supported by the NOESY spectrum of **2**. As in the case of **1**, TDDFT calculations led to the obtainment of calculated ECD spectra. The calculated spectrum of (2*R*,5*S*,6*S*,8*R*,9*R*,10*S*,18*R*,19*S*)-**2** matched the experimental data closely, suggesting a (2*R*,5*S*,6*S*,8*R*,9*R*,10*S*,18*R*,19*S*) absolute configuration for **2**. Compound **2** was therefore elucidated as (2*R*,5*S*,6*S*,8*R*,9*R*,10*S*,18*R*,19*S*)-2-benzoyloxy-6-methoxy-18-butyryloxy-19-acetyloxy-18,19-epoxycleroda-3,13(16),14-triene.

Compound **3** was obtained as a colorless oil. Its HRESIMS showed a molecular ion at *m/z* 485.2512 $[M+Na]^+$ (calcd for $C_{26}H_{38}NaO_7$,

Table 3
Cytotoxicities of compounds **1–5** against three human cancer cell lines (IC_{50} values).

Compound	A549 (μM)	HeLa (μM)	HepG2 (μM)
1	40.8 ± 3.4	> 60	> 60
2	19.7 ± 1.7	12.1 ± 1.1	49.3 ± 3.2
3	> 60	49.4 ± 6.2	> 60
4	18.3 ± 2.5	9.0 ± 1.0	> 60
5	10.2 ± 0.6	5.3 ± 0.2	10.7 ± 0.4
Etoposide[a]	16.5 ± 1.9	25.8 ± 1.9	16.0 ± 2.4

[a] Etoposide was used as a positive control. All results are expressed as the mean ± SD.

485.2515), corresponding to a molecular formula of $C_{26}H_{38}O_7$. The ^1H and ^{13}C NMR spectra indicated that compound **3** has the same cleroodane diterpenoid skeleton as compounds **1** and **2**. The same acetyloxy and methoxy groups as present in compounds **1** and **2** were apparent according to the corresponding proton and carbon signals (Tables 1 and 2). In addition, a propionyloxy group was also deduced and defined from the carbon signals (δ_C 174.0, 27.9, and 9.2) and the corresponding proton signals [δ_H 2.38 (2H, q, J = 7.7 Hz) and 1.17 (3H, t, J = 7.7 Hz)]. The acetyloxy, methoxy, and propionyloxy groups were verified to be located at C-19, C-18, and C-2, respectively, by the corresponding cross-peaks in the HMBC spectrum (Fig. 2). There were no other acyloxy groups in **3** and a hydroxy group was inferred as being attached at C-6, as supported by the chemical shifts of C-6 and the HRESIMS data. The NOESY spectrum indicated the skeletal conformation of compound **3** to be the same as those of compounds **1** and **2**, and the C-2 propionyloxy, the C-18 methoxy, the C-19 acetyloxy, and the C-6 hydroxy groups were all assigned as α-oriented. After defining the relative configuration, an experimental ECD spectrum of **3** was recorded, which was in accordance with the calculated spectrum (Fig. 4C), leading to the assignment of a (2*R*,5*S*,6*S*,8*R*,9*R*,10*S*,18*S*,19*S*) absolute configuration for **3**. Compound **3** was thus characterized as (2*R*,5*S*,6*S*,8*R*,9*R*,10*S*,18*S*,19*S*)-2-propionyloxy-18-methoxy-19-acetyloxy-18,19-epoxycleroda-3,13(16),14-trien-6-ol, named kurziterpene C.

Analysis of the ^1H and ^{13}C NMR spectra of compounds **4** and **5** (kurziterpenes D and E) indicated that both compounds are based on the same scaffold as that of compounds **1–3**. For compound **4**, besides a butyryloxy, a methoxy, and an acetyloxy group, as present in compounds **1–3**, an additional isovaleryloxy group was deduced and supported by the 1D and 2D NMR spectra. The positions of these substituent groups were assigned as shown in Fig. 2 by the corresponding HMBC correlations. For compound **5**, in addition to one acetyloxy and two butyryloxy groups indicated by the proton and carbon signals exhibited (Tables 1 and 2), a hydroxy group was assigned according to the oxygenated carbon signal [δ_C 73.1 (C-6)] and the HRESIMS data. The two butyryloxy groups were found to be located at C-2 and C-18, and the acetyloxy group was located at C-19, on the basis of HMBC correlations as shown in Fig. 2. The hydroxy group was placed at C-6 based on its chemical shift. After determining the planar structures, the same relative configuration for compounds **4** and **5** as those of compounds **1–3** was revealed by the careful analysis of their NOESY spectra, with the substituent groups at C-2, C-6, C-18, and C-19 all in α-positions. On the basis of the same molecular conformations and identical experimental ECD spectra of compounds **3–5**, compounds **4** and **5** were elucidated as (2*R*,5*S*,6*S*,8*R*,9*R*,10*S*,18*R*,19*S*)-2-butyryloxy-6-methoxy-18-isovaleryloxy-19-acetyloxy-18,19-epoxycleroda-3,13(16),14-triene, and (2*R*,5*S*,6*S*,8*R*,9*R*,10*S*,18*R*,19*S*)-2,18-dibutyryloxy-19-acetyloxy-18,19-epoxycleroda-3,13(16),14-trien-6-ol, respectively.

3.2. Cytotoxic activities

Cancer is a serious and huge threat to human health and has been concerned extensively by the public. It is therefore an urgent need to develop new agents to treat cancer effectively. Related studies have shown that the discovery of bioactive natural products plays an

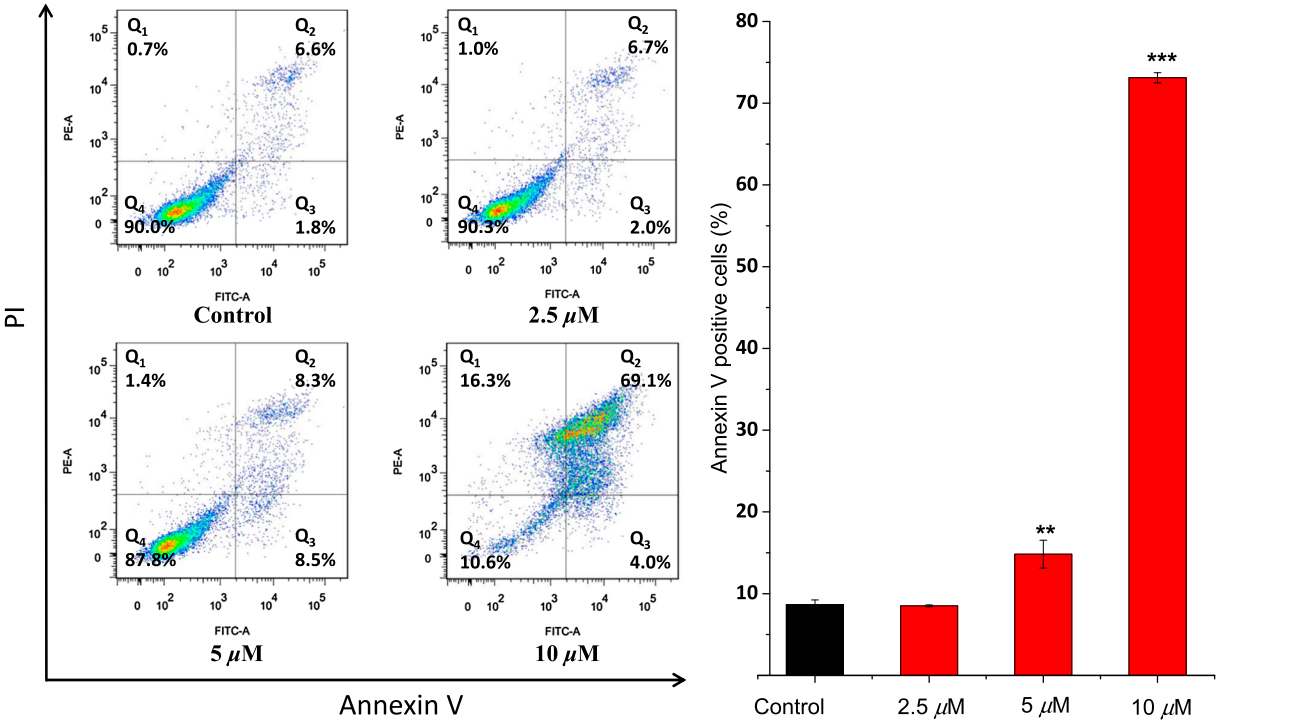

Fig. 5. Apoptosis effects of HeLa cells induced by compound **5**. HeLa cells were treated with different concentrations (2.5, 5, and 10 μM) of compound **5** for 48 h. Then the cells were harvested, stained with Annexin V and propidium iodide (PI), and subsequently analyzed by flow cytometry. (Left) Flow cytometric analysis of HeLa cells treated with different concentrations of compound **5**. (Right) Histogram of apoptotic cells at 48 h with the treatment of compound **5**. (**) $p < 0.01$, (***) $p < 0.001$.

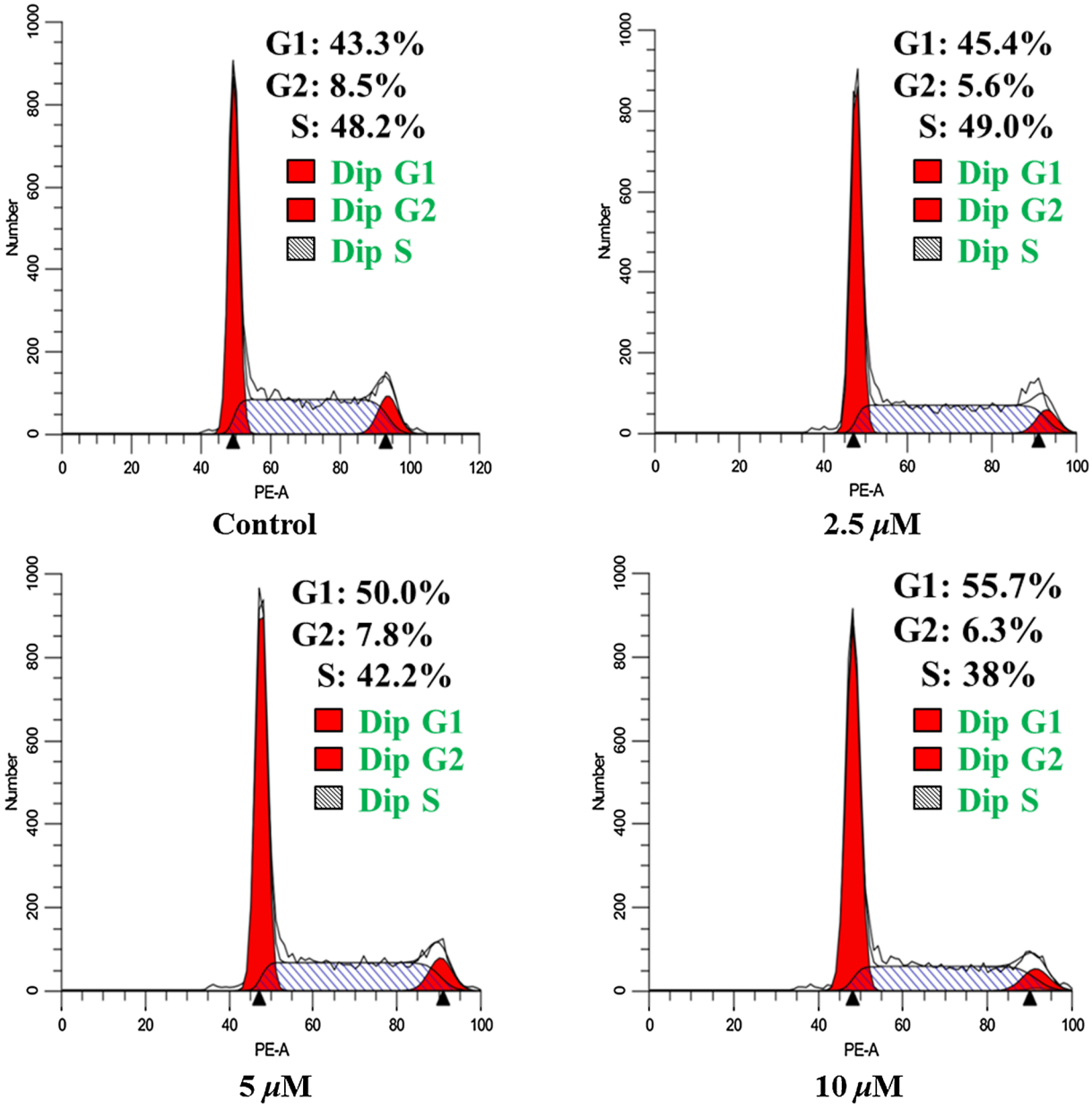

Fig. 6. Arrest effects of **5** on HeLa cell cycle. HeLa cells were treated with different concentrations (2.5, 5, and 10 μM) of compound **5** for 48 h. Then the cells were harvested and stained with propidium iodide (PI), and the cell cycle distribution was analyzed using flow cytometry.

important role in the research and development of new agents to treat cancer [15,16]. To obtain bioactive natural products as lead compounds for cancer, compounds **1**–**5** isolated from the twigs of *C. kurzii* were evaluated for their cytotoxic activities against three cell lines A549, HeLa, and HepG2 cells using a protocol reported previously [17,18]. Etoposide was used as a positive control [19,20]. All of the compounds exhibited cytotoxic effects toward the three cancer cell lines. For human lung cancer A549 cells, compounds **1** and **3** showed weak activities with IC_{50} values more than 40 μM, and compounds **2, 4**, and **5** showed moderate cytotoxic effects with IC_{50} values of 19.7, 18.3, and 10.2 μM, respectively. The IC_{50} values of compounds **2, 4**, and **5** cytotoxic to A549 cells were less than 20 μM and comparable to the positive control etoposide (IC_{50} value, 16.5 μM). For human cervical cancer HeLa cells, compounds **1** and **3** were weakly effective (IC_{50} values > 40 μM), compounds **2** and **4** exhibited moderate effects with IC_{50} values of 12.1 and 9.0 μM. Interestingly, compound **5** showed promising activity with IC_{50} value of 5.3 μM compared to the positive control etoposide (IC_{50} value, 25.8 μM). For human hepatocellular carcinoma HepG2 cells, compound **5** possessed moderate cytotoxicity with an IC_{50} value of 10.7 μM, while the other compounds had weak cytotoxicity (IC_{50} values > 40 μM). These cytotoxic data were collated in Table 3, which revealed that compound **5** was the most active toward three cancer cell lines.

3.3. Apoptosis effects induced by compound 5

All of the compounds were cytotoxic toward the three cancer cell lines and compound **5** seemed to be the most active, especially to HeLa cells. To understand the possible action mechanism of cytotoxicity, compound **5**, the most potent compound, was selected to investigate the apoptosis effects on HeLa cells. The cells were treated with different concentrations (2.5, 5, and 10 μM) of compound **5** for 48 h, and then the cells were harvested, stained with propidium iodide (PI) and Annexin V-FITC, and subsequently analyzed by flow cytometry. As shown in Fig. 5, significant apoptotic effects on HeLa cells induced by compound **5** were observed clearly. With the increase of concentration of

compound **5**, the percentage of apoptotic cells rose from 8.7% (2.5 μM) to 16.8% (5 μM) and 73.1% (10 μM). The data indicated that compound **5** induced apoptosis of HeLa cells in a dose-dependent manner.

3.4. Effects of compound 5 on cell cycle

Apoptosis, or programmed cell death, is intimately coupled to cell cycle progression, which means interruption or arrest of cell cycle [21]. Cell cycle includes generally interphase (G1, S, and G2 phases) and mitosis phase (M phase). Therefore, to better understand cytotoxic mechanism, the effects of compound **5** on the cell cycle distribution of HeLa cells were evaluated. To understand the apoptosis process of HeLa cells induced by compound **5**, cell cycle distribution was evaluated using flow cytometric analysis. After treated with different concentrations (2.5, 5, and 10 μM) of compound **5** for 48 h, the cell proportion in different phases varied following the change of concentrations. Compared to the control, the percentages of the cells in the G0/G1 phase increased markedly and the cells in S phase decreased when treated with the concentration of 10 μM of compound **5** (Fig. 6). These data suggested that compound **5** arrested the HeLa cell cycle at the G0/G1 stage, leading to the cell apoptosis.

4. Conclusion

The present phytochemical investigation on the twigs of *C. kurzii* has led to the isolation of five new clerodane diterpenoids (**1–5**). Their structures were elucidated on the basis of 1D and 2D NMR spectroscopic data analysis, and the absolute configurations of compounds **1–5** were established via comparison of experimental and calculated ECD spectra. All of the isolates were evaluated for their cytotoxic activities toward A549, HeLa, and HepG2 cells. Most diterpenoids showed potent cytotoxicities against the selected cancer cells. Compound **5** showed the most potent cytotoxic effects against HeLa cells with an IC_{50} value of 5.3 μM. The preliminary mechanism studies revealed that compound **5** induced apoptosis and arrested the HeLa cell cycle at the G0/G1 stage to exert cytotoxic effects.

Declaration of Competing Interest

The authors of the present manuscript have declared that no competing interests exist.

Acknowledgments

This work was supported by the National Key Research and Development Program of China (No. 2018YFA0507204), the National Natural Science Foundation of China (Nos. U1703107 and U1801288), Hundred Young Academic Leaders Program of Nankai University, State Key Laboratory for Chemistry and Molecular Engineering of Medicinal Resources (Guangxi Normal University, No. CMEMR2019-B01), and the Fundamental Research Funds for the Central Universities (Nos. 63191142 and 63191731).

Appendix A. Supplementary material

Supplementary data to this article can be found online at https://doi.org/10.1016/j.bioorg.2019.102995.

References

[1] D.J. Newman, G.M. Cragg, J. Nat. Prod. 79 (2016) 629–661.
[2] Editorial Committee of the Flora of China, Chinese Academy of Sciences. Flora of China, Vol. 52 (1), Science Press, Beijing, 1999, pp. 69 − 72.
[3] L. Xia, Q. Guo, P. Tu, X. Chai, Phytochem. Rev. 14 (2015) 99–135.
[4] S. Aimaiti, A. Suzuki, Y. Saito, S. Fukuyoshi, M. Goto, K. Miyake, D.J. Newman, B.R. O'Keefe, K.H. Lee, K. Nakagawa-Goto, J. Org. Chem. 83 (2018) 951–963.
[5] G.M. Vieira-Júnior, T.O. Gonçalves, L.O. Regasini, P.M. Ferreira, C.O. Pessoa, L.V. Costa Lotufo, R.B. Torres, N. Boralle, V.S. Bolzani, A.J. Cavalheiro, J. Nat. Prod. 72 (2009) 1847–1850.
[6] E.L. Whitson, C.L. Thomas, C.J. Henrich, T.J. Sayers, J.B. Mcmahon, T.C. Mckee, J. Nat. Prod. 73 (2010) 2013–2018.
[7] R.B. Williams, A. Norris, J.S. Miller, C. Birkinshaw, F. Ratovoson, R. Andriantsiferana, V.E. Rasamison, D.G. Kingston, J. Nat. Prod. 70 (2007) 206–209.
[8] S. Gibbons, A.I. Gray, P.G. Waterman, Phytochemistry 41 (1996) 565–570.
[9] J. Xu, J. Kang, X. Sun, X. Cao, K. Rena, D. Lee, Q. Ren, S. Li, Y. Ohizumi, Y. Guo, J. Nat. Prod. 79 (2016) 170–179.
[10] J. Xu, F. Ji, X. Sun, X. Cao, S. Li, Y. Ohizumi, Y. Guo, J. Nat. Prod. 78 (2015) 2648–2656.
[11] J. Xu, Q. Zhang, M. Wang, Q. Ren, Y. Sun, D.Q. Jin, C. Xie, H. Chen, Y. Ohizumi, Y. Guo, J. Nat. Prod. 77 (2014) 2182–2189.
[12] MOE 2013.08; Chemical Computing Group Inc., www. chemcomp.com.
[13] T. Bruhn, A. Schaumlöffel, Y. Hemberger, G. Bringmann, SpecDis, Version 1.62, University of Wuerzburg, Germany, 2014.
[14] Gaussian 09, Revision B.01, Gaussian, Inc., Wallingford, CT, 2010.
[15] J.S. Yu, D. Lee, S.R. Lee, J.W. Lee, C.I. Choi, T.S. Jang, K.S. Kang, K.H. Kim, Bioorg. Chem. 76 (2018) 28–36.
[16] S. Gao, D. Sun, G. Wang, J. Zhang, Y. Jiang, G. Li, K. Zhang, L. Wang, J. Huang, L. Chen, Bioorg. Chem. 69 (2016) 121–128.
[17] G.D. Yao, Q. Sun, X.Y. Song, X.X. Huang, Y. Zhang, S.J. Song, Bioorg. Chem. 77 (2018) 619–624.
[18] D.H. Li, J.Y. Li, C.M. Xue, T. Han, C.M. Sai, K.B. Wang, J.C. Lu, Y.K. Jing, H.M. Hua, Z.L. Li, J. Nat. Prod. 80 (2017) 2893–2904.
[19] D. Pertuit, M. Larshini, M.A. Brahim, M. Markouk, A.C. Mitaine-Offer, T. Paululat, S. Delemasure, P. Dutatre, M.A. Lacaille-Dubois, Phytochemistry 139 (2017) 81–87.
[20] H. Mirzaei, M. Shokrzadeh, M. Modanloo, A. Ziar, G.H. Riazi, S. Emami, Bioorg. Chem. 75 (2017) 86–98.
[21] K.L. King, J.A. Cidlowski, Annu. Rev. Physiol. 60 (1998) 601–617.